Supplementary information

“One-pot one-step enzymatic synthesis of 5-(aminomethyl)-2-furancarboxylic acid from 5-(hydroxymethyl) furfural”

Eleonora Fornoni, Ammar Al-Shameri, Pablo Domínguez de María, Volker Sieber

Supplementary information content

1. Abbreviations

ALDH	Aldehyde Dehydrogenase
AMFA	5-aminomethyl-2-furan aldehyde
AMFCA	5-aminomethyl-2-furan carboxylic acid
BsaI	BsaI restriction enzyme
CO	Cut-off
CV	Column Volume
DA-64	N-(-Carb-oxy-methyl-amin-o-carbonyl-)-4,-4'-bis-(-di-methyl-amin-o-)-di-phen-yl-amine Sodium Salt
DAD	Diode Array Detector
DFF	2,5-diformylfuran
dNTPs	Deoxyribonucleotide triphosphate mixture
DTT	Dithiothreitol
E	Elution
FAD	Flavin adenine dinucleotide
FFCA	5-formyl-2-furan carboxylic acid
GWP	Global Warming Potential
HMF	5-(hydroxymethyl)-2-furanaldehyde
HMFCA	5-hydroxymethyl-2-furan carboxylic acid
HMFO	HMF oxidase
HPLC	High-pressure Liquid Chromatography
HRP	Horse-radish peroxidase
IPTG	Isopropyl ß-D-1-thiogalactopyranoside
LB	Lysogeny Broth
LDH	Lactate dehydrogenase
MS	Mass Spectrometry
MW	Molecular Weight
NAD^+/NADH	Nicotinamide adenine dinucleotide (oxidized/reduced)
NEB	New England Biolabs
O/N	Over-night
OD_{600}	Optical Density at 600 nm
PEG-8000	Polyethylen-glycol 8000
PLP	Pyridoxal 5'-phosphate
RW	Resuspension/Wash
SDS-PAGE	Sodium Dodecyl Sulphate – Polyacrylamide Gel Electrophoresis
TLC	Thin Layer Chromatography
ε	Extinction coefficient

2. Materials and methods

2.1 Chemicals and commercial enzymes

All chemicals were purchased from Sigma-Aldrich, Carl Roth or VWR, if not otherwise stated. Analytical standards were purchased from Carl Roth (HMF), Sigma-Aldrich (DFF, FDCA), Tokyo Chemical Industry (HMFCA, FFCA) and abcr GmbH (AMFCA). All molecular biology enzymes were purchased from New England Biolabs (NEB). Lactate dehydrogenase (LDH) was from Karl Roth (art. nr.: 6060.1). Catalase and horseradish peroxidase (HRP) were purchased from Sigma-Aldrich.

2.2 Genes and plasmids

All genes were synthetized by ThermoFisher Scientific (GeneArt Gene Synthesis). Genes were assembled *via* either Golden Gate or Gibson assembly in pET28a backbones with a N-terminus His-tag, if not otherwise stated. All plasmid sequences were confirmed by external Sanger sequencing (Eurofins Genomics). **Table S1** presents a list of all plasmids used in this work.

Table S1. Plasmids specifications.

Enzyme	Original organism	NCBI protein accession nr	Codon optimization	Reference
*Metsp*HMFO	*Methylovorus sp. MP688*	ADQ83320.1	yes	[1]
*Metsp*Q8-HMFO	*Methylophilus sp. Q8*	WP_304413257.1	yes	This work.
*Sk*HMFO	*Stutzerimonas kirkiae*	WP_131187983.1	yes	This work.
*Pc*HMFO	*Pseudomonas citronellolis*	KAF1072365.1	yes	This work.
*Pb*HMFO	*Pseudomonas bohemica*	WP_110950867.1	yes	This work.
*Xa*HMFO	*Xanthobacter autotrophicus*	WP_282638866.1	yes	This work.
MBP-*Mycsp*HMFO (Y444F)	*Mycobacterium sp. MS1601*	AQA01725.1	yes	[2]
Cv-ωTA	*Chromobacterium violaceum*	AAQ59697.1	yes	[3]
*Bs*AlaDH	*Bacillus subtilis*	AAA16038.1	no	[4]
FDH[a]	*Candida bouidinii*	CAA57036.1	yes	[5]
*Ec*ALDH	*Escherichia coli K12*	AAA23428.1	no	[6]
*Bov*ALDH	*Bos taurus (lens)*	AAA74234.1	yes	[7]
*Sph*ALDH	*Sphingobium sp. SYK-6*	BAK67507.1	yes	[8]
*Metsp*HMFO(V367R) [b]	*Methylovorus sp. MP688*	ADQ83320.1 (wt)	yes	[9]
*Lp*NOX	*Lactobacillus pentosus*	ALT83553.1	yes	[10]

[a] Cloned with C-end His-tag.

[b] Gene obtained via PCR amplification of the wild-type gene for *Metsp*HMFO.

2.3 Golden Gate cloning

For Golden Gate assembly, a previously described procedure was followed with some modifications[11]. Plasmids and inserts presented matching BsaI cutting sites at both 5'- and 3'-end. Reaction mixtures were prepared in a 20 µL final volume (adjusted with Milli-Q water) containing: 20 fmol of empty plasmid, 60 fmol of insert, BsaI-HF®v2, T4 DNA ligase, T4 DNA ligase buffer. The reactions were incubated for 2 h at 37 °C and directly used for the transformation of *Escherichia coli* DH5α chemically-competent cells. Cells were grown on LB (Lysogeny Broth)-agar plates supplemented with antibiotic, O/N at 37 °C. One single colony was inoculated in 5 mL LB media with antibiotic and grown with shaking at 37 °C, O/N. The culture was harvested (centrifugation 4000 xg, 4 °C, 15 min) and treated for plasmid extraction with the GeneJET Plasmid Miniprep Kit from ThermoFisher Scientific.

2.4 Gibson assembly

A modified version of the Gibson method[12] was followed. Backbones and inserts were prepared to have two 20 bp over-lapping regions corresponding to the insertion sites. Linearized backbone and insert were mixed in a 1:3 molar ratio (20 fmol of initial backbone) to a 10 µL final volume (adjusted with Milli-Q water). The mixture was then combined to 10 µL of a master-mix containing: 5%(w/v) PEG-8000, 100 mM Tris-Cl pH 7.5 buffer, 10 mM $MgCl_2$, 10 mM DTT (dithiothreitol), 800 mM dNTPs, 1 mM NAD^+, T5 exonuclease, Phusion® High-Fidelity DNA Polymerase, Taq DNA ligase. The reactions were incubated at 50 °C for 1 h. A volume of 10 µL of reaction was used for the transformation of chemically-competent *E. coli* DH5α cells. Cells were grown on LB-agar plates supplemented with antibiotic, O/N at 37 °C. One single colony was inoculated in 5 mL LB media with antibiotic and grown with shaking at 37 °C, O/N. The culture was finally treated for plasmid extraction with the GeneJET Plasmid Miniprep Kit from ThermoFisher Scientific.

2.5 Site-directed mutagenesis of *Metsp*HMFO

In *Metsp*HMFO amino acid sequence the valine (5'-GTT) in position 367 was mutated to an arginine (5'-CGT). The pET28a plasmid carry the gene for *Metsp*HMFO was amplified by PCR using the primers 5'-GGCCAGCGCACGTTTTTGGG (forward) and 5'-

AGACCGCTAACCGGATCTGCACC (reverse). The PCR reaction was prepared in a final volume of 50 µL (adjusted with Milli-Q water) containing 1x Phusion HF buffer (NEB), 200 µM dNTPs, 0.5 µM of each primer, 40 ng of template DNA, 1 U of Phusion® High-Fidelity DNA Polymerase. The reaction was run in a thermocycler following the standard protocol provided by NEB for the polymerase used. The template DNA was then digested with the exonuclease DpnI for 1 h at 37 °C. After DpnI inactivation (20 min, 80 °C), the PCR product was cleaned using the NucleoSpin® Gel and PCR Clean-up kit (Macherey-Nagel), following the standard protocol for PCR clean-up. Subsequently, a ligation reaction was prepared in a final volume of 20 µL (adjusted with Milli-Q water) containing 50 ng of linear DNA, 1x T4 DNA Ligase Buffer (NEB), 1 µL T4 DNA Ligase, 1 µL T4 Polynucleotide Kinase. The reaction was incubated O/N at 4 °C. After enzyme inactivation (20 min, 65 °C), 10 µL of reaction product were used for the thermal transformation of chemically-competent *E. coli* DH5α cells. Cells were grown on LB-agar plates supplemented with kanamycin, O/N at 37 °C. The next day, one single colony was inoculated in 5 mL LB media with kanamycin and grown while shaking at 37 °C, O/N. The culture was finally treated for plasmid extraction with the GeneJET Plasmid Miniprep Kit from ThermoFisher Scientific.

2.6 Enzyme expression and purification

All enzymes were recombinantly expressed in *E. coli* BL21(DE3) cells. A pre-culture was prepared by inoculation of one single colony of cells transformed with the desired plasmid in 25 mL of LB media supplemented with 100 $\mu g \cdot mL^{-1}$ kanamycin. The culture was grown shaking in a baffled-flask at 37 °C, O/N. Main cultures were prepared by inoculation of an opportune volume of pre-culture in 1 L of TB media (Terrific Broth, 12 $g \cdot L^{-1}$ tryptone, 24 $g \cdot L^{-1}$ yeast extract, 5 $g \cdot L^{-1}$ glycerol, 2.31 $g \cdot L^{-1}$ KH_2PO_4, 12.54 $g \cdot L^{-1}$ K_2HPO_4) with antibiotic to a starting $OD_{600} \approx 0.05$. Cultures were grown at 37 °C, shaking in baffled flasks, until $OD_{600} > 0.8$. Protein expression was induced with 0.1-0.5 mM IPTG (isopropyl ß-D-1-thiogalactopyranoside) and the culture was transferred to room temperature (RT, 20-22 °C) and grown for 20 h. Cells were harvested by centrifugation at 8'000 xg, 4 °C, for 15 min.

For protein purification, cell pellets were resuspended in 100 mM NaPi 150 mM NaCl 20 mM imidazole buffer (pH 8.0) supplemented with 10%(v/v) FastBreak™ Cell Lysis Reagent (Promega) and disrupted by sonication for 10 min, on ice. Only when purifying HMFOs and *Lp*NOX, the cell lysates were added with 20 µM of FAD and incubated at 30 °C for 30 min under constant oscillation. Cell debris were removed by centrifugation at 40'000 xg, 4 °C, 30 min. Enzymes of interest were purified from the supernatant on an Äkta Pure system (GE Healthcare) equipped with a HisTrap FF 5mL column (Cytiva). After sample application, the column was washed with 5 column volumes of resuspension buffer. Elution was obtained with an increasing gradient (0-100%) of elution buffer (100 mM NaPi 150 mM NaCl 500 mM imidazole, pH 8.0). Elution fractions corresponding to a UV signal above 50 mAU (arbitrary units) were pooled together and treated for buffer exchange with a HiPrep 26/10 desalting column (Cytiva) equilibrated with 100 mM NaPi 50 mM NaCl buffer (pH 8.0). Elution fractions were collected according to the same criteria used above. For all ALDHs, the eluted enzyme solutions were supplemented with 5%(v/v) glycerol before storage. Final enzyme solutions were fast frozen by direct dropping in liquid nitrogen and stored at -80 °C.

2.7 Protein quantification

ALDHs, CbFDH and BsAlaDH solutions were quantified with a NanoPhotometer P-Class P300 (Implen). HMFOs and Cv-ωTA solutions were quantified *via* Bradford Assay using ROTI®Quant solution (Karl Roth) and following the protocol for 96-well plates in its user manual.

2.8 SDS-PAGE (Sodium Dodecyl Sulphate – Polyacrylamide Gel Electrophoresis) analysis

SDS-PAGE samples were prepared by the addition of 1x SDS-PAGE loading dye (25%(v/v) glycerin, 12.5%(v/v) β-mercaptoethanol, 7.5%(w/v) SDS sodium salt, 0.25 M Tris base pH 6.8, 0.25 $g \cdot L^{-1}$ bromophenol blue) to protein solutions and boiling at 95 °C for 10 min. The samples were loaded on 12% polyacrylamide SDS-PAGE gels, which were developed under constant voltage (120 V) for 60 min. Staining was performed with a Comassie-based staining solution (0.1 $g \cdot L^{-1}$Comassie G250 in 0.1% HCl in ddH_2O).

2.9 HMFOs activity assay

HMFO activities were quantified *via* hydrogen peroxide detection with horse-radish peroxidase (HRP) and the dye DA-64 (N-(-Carb-oxy-methyl-amin-o-carbonyl-)-4,-4'-bis-(-di-methyl-amin-o-)-di-phen-yl-amine Sodium Salt)[13]. Assay reactions were prepared in 100 mM NaPi buffer (pH 8.0) and generally contained: 5 mM substrate, 5 U/mL HRP, 50 µM DA-64 and an adequate amount of the specific HMFO tested. The assays were performed in 96-well plates and started by substrate addition. The absorbances at 540 nm and 727 nm were followed for 30 min at 30 °C. To calculate the activity, the absorbance difference at 727 nm and 540 nm was converted to moles of Bindschedler's green (product formed from DA-64 oxidation with HRP) using a measured extinction coefficient of 76500 $M^{-1} \cdot cm^{-1}$. One unit of enzymatic activity (1 U) was defined as the amount of enzyme needed for the oxidation of 1 µmol of DA-64 per minute.

For enzyme kinetics, the assays were performed on a substrate range of 0-10 mM for DFF and 0-40 mM for HMF, FFCA and HMFCA.

2.10 NADH assays

The detection of NADH formation/consumption *via* absorbance was used for the quantification of the enzymatic activities of *Cb*FDH, *Bs*AlaDH, *Cv*-ωTA and each ALDH. The compositions of the assay reactions for each enzyme are indicated in the table below (**Table S2**).

Table S2. Compositions of NADH assay solutions used for enzymatic activity determination of different enzymes.

	***Cb*FDH**	***Bs*AlaDH**	***Cv*-ωTA**	**ALDHs**
Component	**Concentration in assay solution**			
Substrate	30 mM (formate)	5 mM (pyruvate)	2 mM (FFCA)	5 mM (HMF)
NAD^+	0.5 mM	-	-	1 mM
NADH	-	0.3 mM	0.5 mM	-
Enzyme	min 0.3 µM	min 0.02 µM	min 0.1 µM	(ALDH specific)
NH_4Ac	-	200 mM	-	-
L-alanine	-	-	20 mM	-
PLP (pyridoxal 5'-phosphate)	-	-	0.5 mM	-
LDH (lactate dehydrogenase)	-	-	50 U/mL	-

For activity determinations, reactions were prepared in 100 mM NaPi buffer (pH 8.0) according to the concentrations above. Reactions were started by substrate addition and the absorbance at 340 nm was followed for 30 min at 30 °C. The extinction coefficient used for NADH for activity calculations was 6220 $M^{-1}\cdot cm^{-1}$. One unit of enzymatic activity (1 U) was defined as the amount of enzyme needed for the formation/consumption of 1 µmol of NADH per minute.

For ALDH enzyme kinetics, the substrate concentrations tested were 0-20 mM for DFF and 0-60 mM for HMF and FFCA. *Cv*-ωTA kinetics were tested on 0-10 mM substrate concentrations.

2.11 HMFCA Cascade reactions

Cascade reactions were generally prepared in 100 mM NaPi buffer (pH 8.0) in a 1 mL final volume in 15 mL reaction tubes. Reaction compositions were as indicated in **Table S3**.

Table S3. Reaction compositions of reactions for HMFCA conversion to AMFCA.

Reaction results in	**Figure S2a**	**Figure S2b**	**Figure 1a**	**Figure 1b**
Component	**Final concentration**			
HMFCA	50 mM	40 mM	20 mM	50 mM
L-alanine	50 mM	50 mM	50 mM	50 mM
PLP (pyridoxal 5'-phosphate)	1 mM	1 mM	2 mM	0.02 mM
NADH	0.2 mM	0.2 mM	0.2 mM	0.5 mM
NH_4 -acetate	300 mM	100 mM	100 mM	280 mM
Na-formate	300 mM	100 mM	100 mM	280 mM
*Cb*FDH	1.65 µM	1.65 µM	1.65 µM	1.65 µM
*Bs*AlaDH	0.57 µM	0.57 µM	0.57 µM	0.55 µM
Cv-ωTA	1.16 µM	0.58 µM	0.58 µM	9.53 µM
*Metsp*HMFO	3.15 µM	4.19 µM	4.19 µM	5.77 µM
Catalase	1 U/mL	1 U/mL	1 U/mL	5 U/mL

After substrate addition, the reactions were left oscillating on a rocking shaker for 24 h at 30 °C. Time samples were taken by centrifugation (20000 xg, 5 min, RT) of reaction solution (50 µL) on 10 kDa CO (cut-off) centrifugal filters (VWR). Samples were then opportunely diluted in ddH_2O and analyzed on HPLC.

2.12 HMF cascade reactions

Cascade reactions were generally prepared in 100 mM NaPi buffer (pH 8.0) in a 1 mL final volume in 15 mL reaction tubes. Reaction compositions were as indicated in **Table S4**. After substrate addition, the reactions were tilted on a rocking shaker for 24 h at 30 °C.

Time samples were taken by centrifugation (20000 xg, 5 min, RT) of reaction solution (50 µL) on 10 kDa CO centrifugal filters (VWR). Samples were then opportunely diluted in ddH_2O and analyzed on HPLC.

Table S4. Reaction compositions of reactions for HMF conversion to AMFCA.

Reaction results in	**Figure 2d**	**Figure 2a-2b-2c**	**Figure S3a-S3b-S3c**	**Figure S4a-S4c-S4d**
Component				**Final concentration**
HMF	18 mM	18 mM	45 mM	45 mM
L-alanine	50 mM	50 mM	50 mM	50 mM (S4a) 25 mM (S4c-S4d)
Na-pyruvate	-	-	-	0 mM (S4a) 25 mM (S4c-S4d)
PLP	0.02 mM	0.01 mM	0.04 mM	0.02 mM
NAD^+/NADH	0.2 mM (NADH)	0.5 mM (NAD^+)	0.5 mM (NAD^+)	0.5 mM (NAD^+)
NH_4 -acetate	100 mM	80 mM	80 mM	100 mM
Na-formate	100 mM	-	-	-
*Cb*FDH	1.66 µM	-	-	-
*Bs*AlaDH	0.57 µM	0.68 µM	0.68 µM	1.63 µM
Cv-ωTA	0.58 µM	1.61 µM	1.61 µM	1.61 µM
*Metsp*HMFO	1.53 µM	0.33 µM	0.33 µM	0.40 µM (S4a-S4d) 0.33 µM (S4c)
Catalase	5 U/mL	5 U/mL	5 U/mL	5 U/mL
ALDH	-	6.66 µM (*Ec*ALDH) 6.51 µM (*Bov*ALDH) 6.28 µM (*Sph*ALDH)	6.66 µM (*Ec*ALDH) 6.51 µM (*Bov*ALDH) 6.74 µM (*Sph*ALDH)	8.99 µM (*Sph*ALDH)

2.13 HMF to AMFCA cascade scale-up

AMFCA production at higher scale was set-up in a 500 mL gas wash bottle with filter plate (porosity 1 - 100–160 µm) covered by aluminum foil (to protect enzymes from light inactivation). A water-moisturized air flow was guaranteed at a constant flow of 15 $mL \cdot min^{-1}$. A temperature of 30 °C was maintained through immersion in a water bath. Stirring at 120 rpm was achieved through a magnetic stirrer inside the solution. The reaction was prepared in a final volume of 50 mL in 100 mM NaPi buffer pH 8.0. The reaction composition was: 46 mM HMF, 50 mM L-Ala, 20 µM PLP, 500 µM NAD^+, 80 mM NH_4-acetate, 1.3 µM *Bs*AlaDH, 2.45 µM *Cv*-ωTA, 0.19 µM *Metsp*HMFO(V367R), 6.76 µM *Sph*ALDH, 5 U/mL catalase. The reaction was monitored for 48 h. Time samples were taken by centrifugation (20000 xg, 5 min, RT) of reaction solution (100 µL) on 10 kDa CO centrifugal filters (VWR). Samples were opportunely diluted in ddH_2O for HPLC analysis. After 48 h, the reaction solution was collected by centrifugation on 10 kDa CO Amicon® Ultra Centrifugal Filters (3000 xg, 20 min, RT).

2.14 AMFCA purification

For AMFCA purification, the harvested reaction solution (from HMF to AMFCA scale-up) was loaded on a pre-equilibrated DOWEX 50WX8 (mesh 200-400) column. The column was washed with 4 CVs of ddH_2O and the compounds of interest were eluted with 4 CVs of 0.5 M ammonia solution. The column was regenerated with 4 CVs of ddH_2O. The elution fractions were analyzed via TLC and the ones co-containing L-Ala and AMFCA were pooled together and dried via rotary evaporation. After complete drying, the obtained powder was resuspended in 100 mM NaPi buffer pH 8.0 to a final concentration of 6.71 $mg \cdot mL^{-1}$. The solution was added with 390 µM NAD^+, 20.3 µM *Bs*AlaDH and 6.26 µM *Lp*NOX. To achieve full deamination of L-Ala to pyruvate, the reaction was incubated at 30 °C for 3 h, under constant oscillation at 30 rpm on a rocking shaker. The reaction solution was collected by centrifugation on 10 kDa CO Amicon® Ultra Centrifugal Filters (3000 xg, 20 min, RT). After harvesting, the solution was loaded again on a pre-equilibrated DOWEX 50WX8 (mesh 200-400) column. The purification on the cation exchanger was performed as mentioned above. After elution, the fractions containing AMFCA were pooled together and dried in a rotary evaporator. The obtained powder was analyzed via LC/MS.

2.15 TLC (Thin Layer Chromatography) analysis

To analyze amine-containing solutions, TLC silica gel 60 F_{254} plates were used. The mobile phase was *n*-butanol:water:methanol:trimethylamine (64:25:10:1). The plates were firstly visualized under UV light and secondly stained with a solution of 0.5% (w/v) ninhydrine in 1% (v/v) acetic acid in *n*-butanol. The plates were heated for 3-5 min at 90 °C to observe color development in correspondence of amine spots.

2.16 HPLC, LC-MS analysis

Samples were analyzed on a Dionex UltiMate 3000 RS HPLC system equipped with a diode array detector (DAD) and a Restek Force Biphenyl column (particles size 1.8 µm, length 100 mm, diameter 2.1 mm). Solvent A was 0.1%(v/v) formic acid in ddH_2O and solvent B was 0.1%(v/v) formic acid in acetonitrile. Elution profile: 100% A for 1 min, increase to 7% B in 2 min, hold for 1 min, increase to 50% B in 2 min, decrease to 0% B in 0.1 min, hold for 4.9 min. Samples were prepared in ddH_2O to a final compound concentration of 20 µM. The compounds of interest were detected at 210 nm (HMFA) and 255 nm (HMF, AMFA, HMFCA, FFCA, FDCA, AMFCA). A typical elution profile for standards is represented in **Figure S6**. For mass spectrometry (MS) analysis, an ESI ion trap unit (Esquire HCT, Bruker) was combined to UV detection. A reference LC-MS chromatogram and AMFCA MS profile are represented in **Figure S12**.

2.17 E-factors and Global Warming Potential (GWP) calculations

Mass E-factors were calculated as kg of waste per kg of product obtained, estimating the reaction media as the main contributing fraction, in the form of wastewater (containing chemicals). GWPs for the upstream process (UPS) for AMFCA productions were calculated according to previously defined equations[14]. Considering a production range of 5-20 $g\ L^{-1}$ AMFCA, both the mass impact (wastewater) and the energy contribution were considered for the calculation of the total GWP. The equation used to calculate the mass impacts was:

$$GWP(wastewater) = \frac{f \cdot \%WaterTreated}{Conv \cdot [SL]} \quad (1)$$

Where *%WaterTreated* corresponds to the part of the water effluent treated. *Conv* stands for the conversion of substrate to final product. *[SL]* represents the substrate loading. And *f* is a constant corresponding to a specific value depending on the wastewater treatment adopted. In the present case *%WaterTreated* was set to 100%. For the assessments, the substrate was considered to be fully converted to AMFCA (*Conv* = 100%). The substrate loading was varied in the range 5-20 $g\ L^{-1}$. The constant *f* was: 0.073 for

wastewater direct treatment in Wastewater Treatment Plant (WWTP), 0.35 for the "recommended" path (wastewater subjected to some pre-treatment steps to remove hazardous chemicals that are incinerated), and 0.63 for the full incineration of the wastewater.

For the calculation of the energy contribution on the total GWP, the AMFCA production was considered to be performed at a constant temperature of 30 °C, for a time of 24 h and given a room temperature of 20 °C. The environmental impact of the energy was calculated with a similar equation to the one above[14]. The equation considers both the energy needed to heat a reactor tank with water up to the reaction temperature and the energy needed to keep the reactor at that temperature for the hours of the reaction. The equation is:

$$GWP(energy\ impact) = \left(\frac{0.037 \cdot \Delta T}{Conv \cdot [SL]}\right) + t \cdot \left(\frac{0.0056 \cdot \Delta T}{Conv \cdot [SL]}\right) \quad (2)$$

Where t corresponds to the reaction time. ΔT is the difference of temperature between the reaction conditions and the room temperature.

GWPs were calculated also for the different steps of the downstream process (DSP) followed for AMFCA isolation. For the water evaporation steps the GWP were calculated assuming a distillation procedure to obtain 1 kg of AMFCA after evaporation. The equation applied was:

$$GWP(distillation) = Q \cdot 1.25 \cdot 0.25\ kg\ CO_2 \cdot kW^{-1} \cdot h^{-1} \quad (3)$$

Where *Q* is the energy needed for the distillation. The factor x1.25 is introduced to penalize for a 25% extra energy needed due to the system lack of ideal behavior. And 0.25 kg $CO_2 \cdot kW^{-1} \cdot h$ is the amount of CO_2 produced per $kW \cdot h^{-1}$ assuming the current European energy production[15]. *Q* was in turn calculated as the amount of energy needed to evaporate a defined mass of water (*m*) according to the formula:

$$Q = m \cdot C_p \cdot \Delta T + m \cdot \Delta H \quad (4)$$

In the equation, the specific heat capacity (C_p) of water was considered (4.184 $kJ \cdot kg^{-1} \cdot °C^{-1}$). The impact of the enthalpy of water vaporization was also taken into account (ΔH = 2260 $kJ \cdot kg^{-1}$). ΔT corresponded to the difference between RT (20 °C) and the water distillation temperature (100 °C). The mass of water to be evaporated was calculated considering a final production of 1 kg of AMFCA.

The GWPs corresponding to the wastewater treatment of effluents from the chromatographic purification were calculated considering a direct treatment in WWTP. Thus, the applied equation was:

$$GWP(chromatography) = 0.073\ \cdot kg\ water \quad (5)$$

Where 0.073 is the constant to be applied to consider the CO_2 production per kg of water treated through mild WWTP.

The GWP of the L-Ala enzymatic degradation was calculated according to equation (2). A reaction temperature of 30 °C and a reaction time of 3 h were evaluated.

3. Supplementary tables

Table S5. Specifications of HMFO enzymes studied in this work.

Enzyme abbreviation	Organism	Accession number [a]	Sequence similarity to MetspHMFO	Purification tag	Reference
*Metsp*HMFO	*Methylovorus sp. MP688*	E4QP00.1	100%	N-end His-tag	[1]
*Metsp*Q8-HMFO	*Methylophilus sp. Q8*	WP_304413257.1	70.13%	N-end His-tag	This work
*Sk*HMFO	*Stutzerimonas kirkiae*	WP_131187983.1	63.38%	N-end His-tag	This work
*Pc*HMFO	*Pseudomonas citronellolis*	KAF1072365.1	63.35%	N-end His-tag	This work
*Pb*HMFO	*Pseudomonas bohemica*	WP_110950867.1	60.98%	N-end His-tag	This work
*Xa*HMFO	*Xanthobacter autotrophicus*	WP_282638866.1	46.10%	N-end His-tag	This work
MBP-*Mycsp*HMFO (Y444F)	*Mycobacterium sp. MS1601*	AQA01725.1	35.21%	N-end His-tag + MBP-tag	[2]

[a] NCBI accession numbers to amino acid sequences.

Table S6. Kinetic parameters of tested HMFOs. Enzymatic activities were measured with a horseradish peroxidase (HRP) coupled assay for H_2O_2 detection. The kinetics were performed in 100 mM NaPi buffer pH 8.0, 30 °C, substrate range 0-10/40 mM.

Enzyme	Substrate	K_M [mM]	k_{cat} [s^{-1}]	k_{cat}/K_M [$M^{-1} s^{-1}$]	K_i [mM]
***Metsp*HMFO**	HMF	0.42 ± 0.38	4.36 ± 0.98	10334.58	n.d.
	DFF	0.64 ± 0.25	0.56 ± 0.05	883.01	n.d.
	FFCA	15.83 ± 2.87	0.01 ± 0.00	0.55	n.d.
	HMFCA	2.62 ± 0.88	4.20 ± 0.67	1602.77	n.d.
MBP-*Mycsp*HMFO (Y444F)	HMF	0.01 ± 0.02	0.14 ± 0.01	11314.42	12.35 ± 4.01
	DFF	n.d.	n.d.	n.d.	n.d.
	FFCA	n.d.	n.d.	n.d.	n.d.
	HMFCA	1.26 ± 0.19	0.20 ± 0.00	155.85	n.d.
***Pc*HMFO**	HMF	0.43 ± 0.04	1.59 ± 0.07	3692.16	n.d.
	DFF	1.55 ± 0.32	0.67 ± 0.10	429.53	22.21 ± 13.92
	FFCA	2.10 ± 0.42	0.04 ± 0.00	19.08	n.d.
	HMFCA	5.14 ± 1.04	2.47 ± 0.30	481.73	36.25 ± 10.08

n.d. = not detected

Table S7. Literature reported kinetic parameters for *Metsp*HMFO and *Mycsp*HMFO.

Enzyme	Substrate	K_M [mM]	k_{cat} [s^{-1}]	k_{cat}/K_M [$M^{-1} s^{-1}$]	K_i [mM]	Reference
***Metsp*HMFO**	HMF	1.4	9.9	7100	n.r.	[1]
	DFF	1.7	1.6	940	n.r.	[1]
	FFCA	n.d.	n.d.	<10	n.r.	[1]
	HMFCA	73	8.5	120	n.r.	[1]
***Mycsp*HMFO (Y444F)**	HMF	1.9	652	342000	n.r.	[2]
	DFF	n.r.	n.r.	n.r.	n.r.	[2]
	FFCA	n.r.	n.r.	n.r.	n.r.	[2]
	HMFCA	n.r.	n.r.	n.r.	n.r.	[2]

n.d. = not detected.
n.r. = not reported

The kinetic parameters obtained in this work for *Metsp*HMFO (**Table S6**) are comparable to previously measured values (**Table S7**), if we account for the differences in experimental conditions[1]. The data collected for MBP-*Mycsp*HMFO(Y444F) on HMF (**Table S6**) are in significant disagreement with previously published values[2] (**Table S7**). However, a non-MBP-tagged *Mycsp*HMFO(Y444F) was used in the previous study and the assay conditions were broadly dissimilar to ours.

Table S8. Measured kinetic parameters for *Cv*-ωTA.

Enzyme	Substrate	K_M [mM]	k_{cat} [s^{-1}]	k_{cat}/K_M [$M^{-1} s^{-1}$]	K_i [mM]
***Cv*-ωTA**	HMF	1.36 ± 0.18	1.40 ± 0.07	1032.64	n.d.
	DFF	1.05 ± 0.21	2.41 ± 0.37	2299.73	2.20 ± 0.66
	FFCA	0.97 ± 0.22	1.83 ± 0.22	1889.29	8.63 ± 2.39
	HMFCA	n.d.	n.d.	n.d.	n.d.

n.d. = not detected.

Table S9. Kinetic parameters of *Mestp*HMFO(V367R). Enzymatic activities were measured with a horseradish peroxidase (HRP) coupled assay for H_2O_2 detection. The kinetics were performed in 100 mM NaPi buffer pH 8.0, 30 °C, substrate range 0-10/40 mM.

Enzyme	Substrate	K_M [mM]	k_{cat} [s^{-1}]	k_{cat}/K_M [M^{-1} s^{-1}]	K_i [mM]
***Metsp*HMFO(V367R)**	HMF	0.50 ± 0.07	4.31 ± 0.22	8661.03	63.16 ± 15.05
	DFF	0.91 ± 1.40	0.60 ± 0.79	665.01	0.26 ± 0.41
	FFCA	1.76 ± 0.81	0.055 ± 0.013	31.27	n.d.
	HMFCA	0.54 ± 0.15	9.68 ± 0.81	17915.84	n.d.

n.d. = not detected

4. Supplementary figures

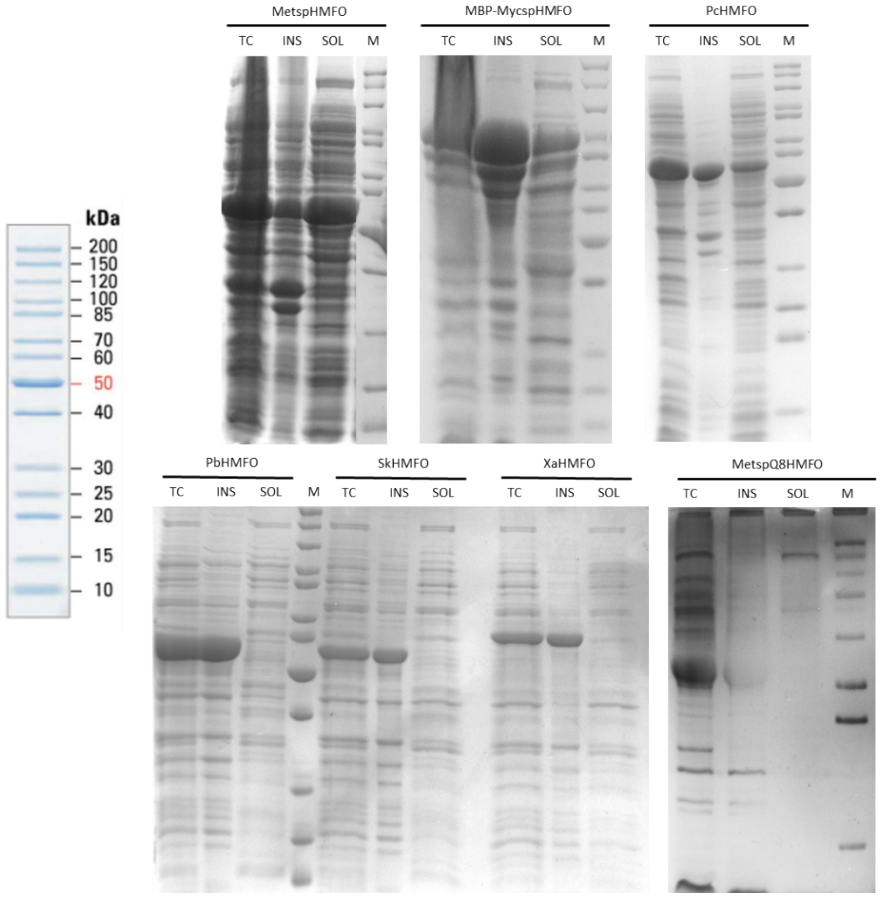

Figure S1. SDS-PAGE gels of expressed HMFOs. M: marker, TC: total cell, INS: insoluble fraction, SOL: soluble fraction. For the analysis, cell pellets were resuspended in 100 mM NaPi pH 8.0 buffer to a 10%(w/v) concentration. Cells were disrupted by sonication in 2 mL reaction tubes (80% amplitude, 0.5 cycle, 5x 1 min sonication and 1 min on ice). The cell lysates (TC fractions) were then centrifuged at 20000 xg, for 30 min, 4 °C. The supernatant was collected as SOL fraction and the pellet was resuspended in the same volume of buffer and collected as INS fraction.

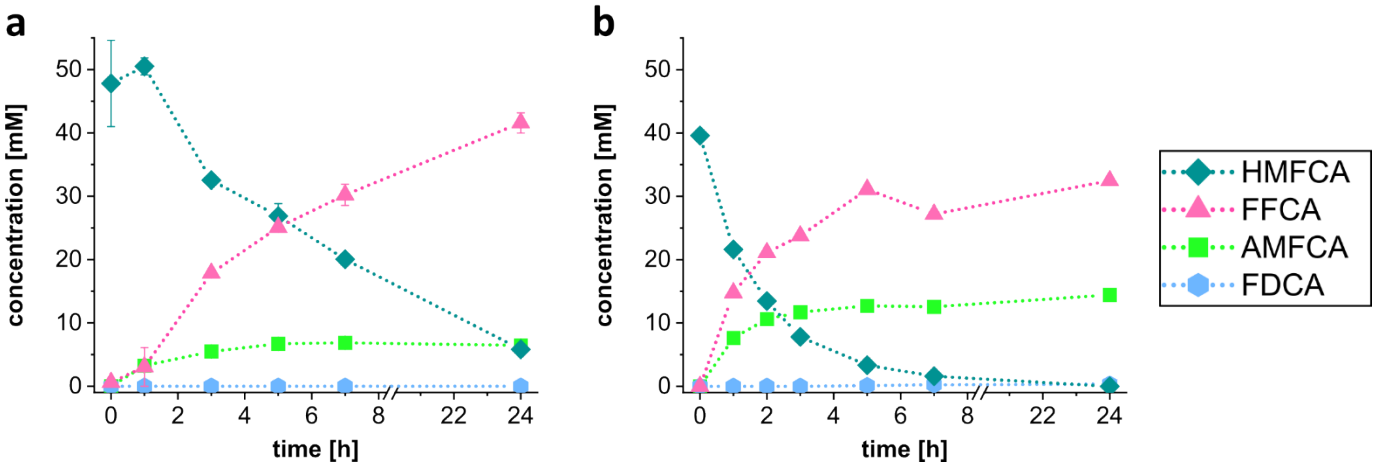

Figure S2. HMFCA conversions to AMFCA with 50 mM (a) and 40 mM (b) initial substrate concentration. Reactions were performed in 100 mM NaPi buffer, pH 8.0, 30 °C, under constant oscillation. The enzyme concentrations used are listed in Table S3.

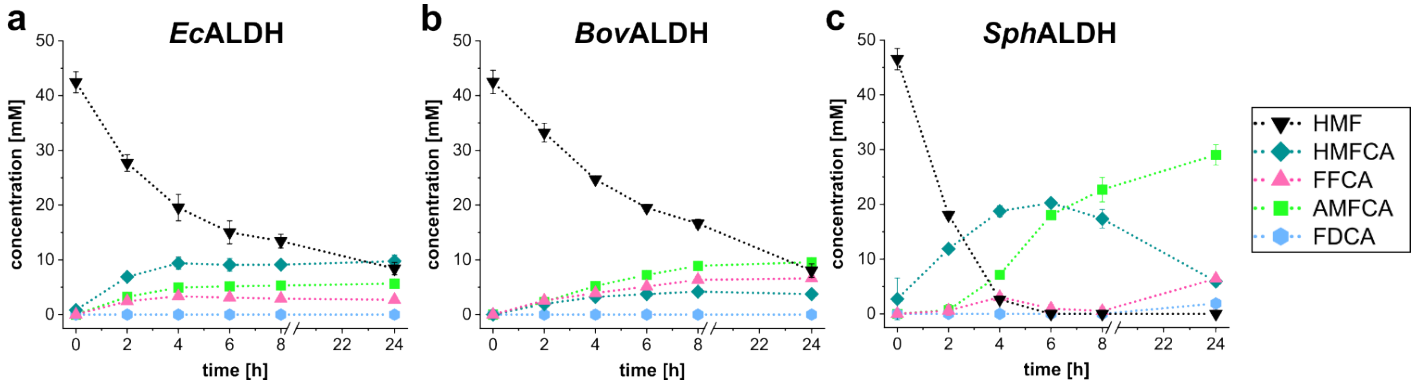

Figure S3. Time courses of 45 mM HMF conversions to AMFCA using different ALDHs: *Ec*ALDH (a), *Bov*ALDH (b), *Sph*ALDH (c). Reactions were performed with 50 mM L-Ala in 100 mM NaPi buffer pH 8.0, 30 °C, under constant oscillation. Enzyme concentrations: 0.33 µM *Metsp*HMFO, 6.66 µM *Ec*ALDH (a), 6.51 µM *Bov*ALDH (b), 6.74 µM *Sph*ALDH (c), 1.61 µM *Cv*-ωTA, 0.68 µM *Bs*AlaDH. Details in **Table S4**.

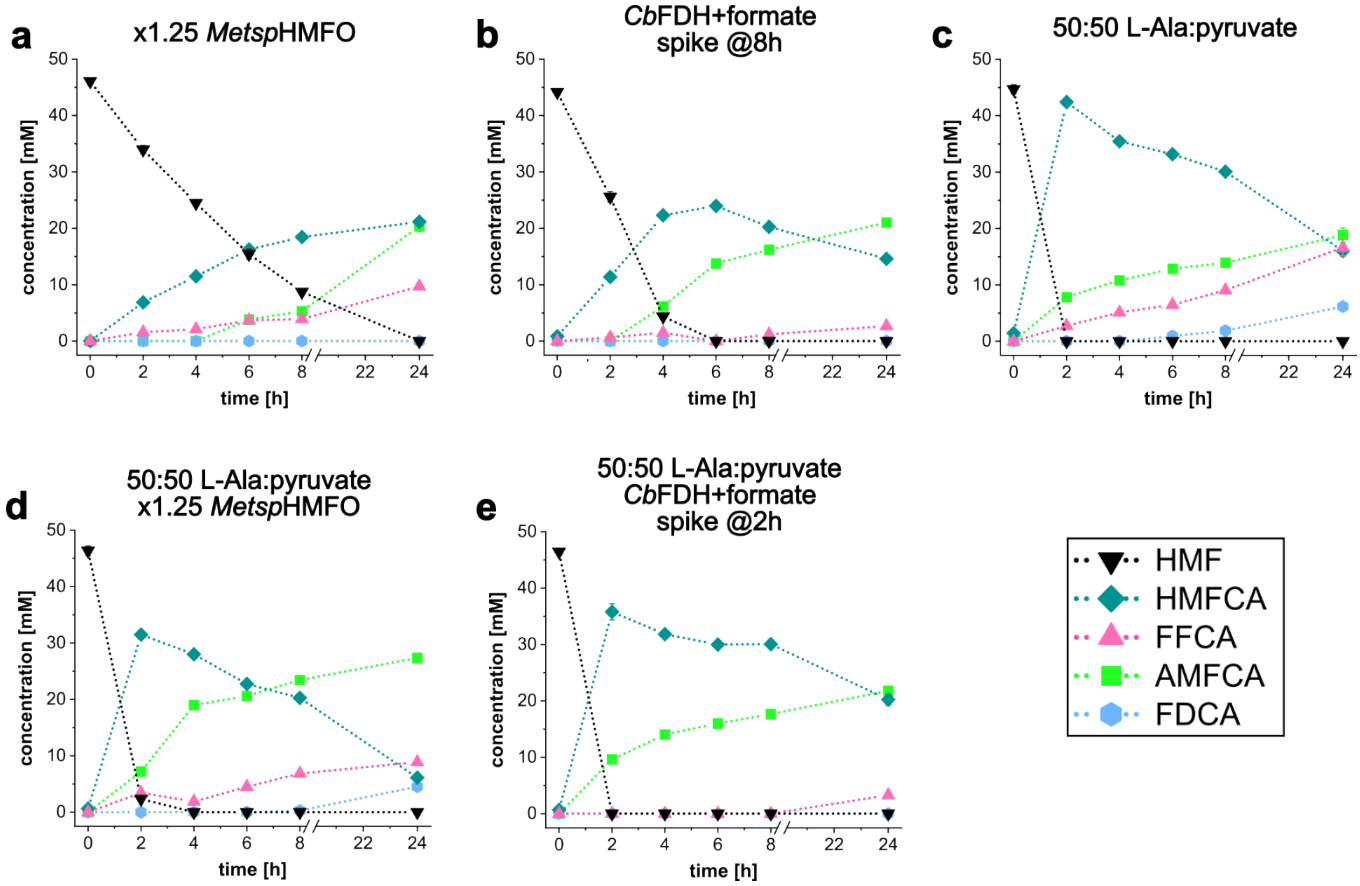

Figure S4. 45 mM HMF conversions to AMFCA in different conditions. Reactions were performed in 100 mM NaPi buffer, pH 8.0, 30 °C, under constant oscillation. The reaction details are reported in Table S4.

As the conversion of 45 mM HMF to AMFCA with the enzymatic cascade proposed in **Scheme 2** resulted in ~62% yield in 24 h even when *Sph*ALDH was included as catalyst (**Figure S3c**), some reaction engineering strategies were tried to obtain better conversions. The results are shown in **Figure S4**. The reference reaction (**Figure S3c**) was performed in 100 mM NaPi buffer pH 8.0, at 30 °C, with 45 mM HMF, 50 mM L-Ala, 0.5 mM NAD^+, 80 mM ammonium acetate, 0.04 mM PLP and 5 $U \cdot mL^{-1}$ catalase. The enzyme concentrations were: 0.33 µM *Metsp*HMFO, 6.74 µM *Sph*ALDH, 1.61 µM *Cv*-ωTA and 0.68 µM *Bs*AlaDH. In the reference reaction, an accumulation of carbon in HMFCA was suspected to hinder AMFCA production, thus a reaction with a higher molar concentration of *Metsp*HMFO (x1.25 compared to reference) was tested in order to accelerate HMFCA oxidation to FFCA. The results (**Figure S4a**) show that intermediate and product formations and HMF consumption were all slowed. We assume that, given *Metsp*HMFO promiscuity, the oxidase most probably yielded a high amount of DFF from the beginning of the reaction and thus all biocatalysts were strongly inhibited and/or cross-linked. Another limitation encountered in the reference was the accumulation of FFCA and FDCA after 8 h of reaction, probably as a result of a slow FFCA amination to AMFCA, in turn due to a slow NAD^+ reduction. Therefore, the tried engineering strategy was the addition of 1.75 µM *Cb*FDH and 100 mM sodium formate after 8 h of reaction to guarantee NADH regeneration

independently from *Sph*ALDH catalysis. The results (**Figure S4b**) suggest a better NADH recirculation: after 24 h, no FDCA was formed and FFCA accumulated to a much lower amount compared to the reference. Still, a yield of only ~47% AMFCA was achieved. The limiting factor can be again traced back to a slow HMFCA oxidation by *Metsp*HMFO as ~32% of the initial HMF was still locked in HMFCA. Another drawback identified in the reference was DFF formation, thus we tried using a 50:50 mixture of L-Ala and pyruvate at the beginning of the reaction, so to favor HMF oxidation by *Sph*ALDH by guaranteeing a fast NAD^+ regeneration by *Bs*AlaDH. The results (**Figure S4c**) show that 45 mM of HMF were efficiently converted to ~36 mM of HMFCA within the first few hours of reaction. However, after 2 h, other limitations became evident as HMFCA was very slowly consumed and FFCA, AMFCA and FDCA all accumulated. Firstly, *Metsp*HMFO represented again a bottleneck for the slow oxidation of HMFCA. Secondly, after fluxing almost all carbon to HMFCA, the NADH regeneration, fundamental for L-Ala recirculation, was not performed anymore by *Sph*ALDH. Thus, L-Ala was consumed for FFCA amination by *Cv*-ωTA, but it was not recirculated fast enough by *Bs*AlaDH. As a consequence, L-Ala concentration decreased to approach its K_M for *Cv*-ωTA (~24 mM for FFCA amination) and this ultimately resulted in a slowed catalysis of FFCA amination to AMFCA. As a confirmation of the imbalance in NADH regeneration, FDCA was again generated, probably by *Sph*ALDH providing for NAD^+ reduction. Further, combinations of the engineering approaches were tried in order to simultaneously profit from the advantages of the single strategies. An initial 50:50 mixture of L-Ala and pyruvate was tested with a higher *Metsp*HMFO concentration (x1.25 the molarity in the reference conditions) in order to accelerate HMFCA oxidation after its initial high accumulation. However, the results (**Figure S4d**) do not highlight a much faster HMFCA oxidation, but rather a lower carbon flux to HMFCA. Apparently, a higher *Metsp*HMFO concentration had a stronger effect on HMF oxidation to DFF rather than HMFCA to FFCA. Still, the reaction ultimately brought to a ~58% conversion to AMFCA, higher than when both strategies were separately implemented (**Figure S4a**, **Figure S4c**). This might be the result of a reduced imbalance in NADH regeneration compared to the reaction in **Figure S4c**. In fact, when DFF is produced, it is then aminated to AMFA and *Sph*ALDH catalyzes its oxidation to AMFCA, thus re-establishing an efficient NAD^+ reduction even after HMF has been fully converted. In another experiment, the initial 50:50 L-Ala:pyruvate mixture was tested together with *Cb*FDH and formate addition after 2 h of reaction to favor AMFCA production by guaranteeing an efficient NADH regeneration after all carbon is fluxed to HMFCA. From the reaction time course (**Figure S4e**), it appears that NADH was efficiently recirculated all along the reaction time, as FFCA accumulated up to only ~3 mM and FDCA did not form at all. Still, AMFCA final yield was only ~46% and ~43% of the initial HMF was stored in HMFCA, highlighting again the slow HMFCA oxidation by *Metsp*HMFO.

Overall, the explored reaction engineering strategies highlighted that the main bottlenecks are intrinsic to the specific biocatalysts employed (for their broad promiscuity) and the cascade design (for NADH regeneration). Higher yields than in the reference reaction (results in **Figure S3c**) were not achieved. Moreover, each of the strategies implies a more expensive processes, as higher amounts of enzymes are employed, carbon dioxide is produced and/or the more expensive pyruvate is used.

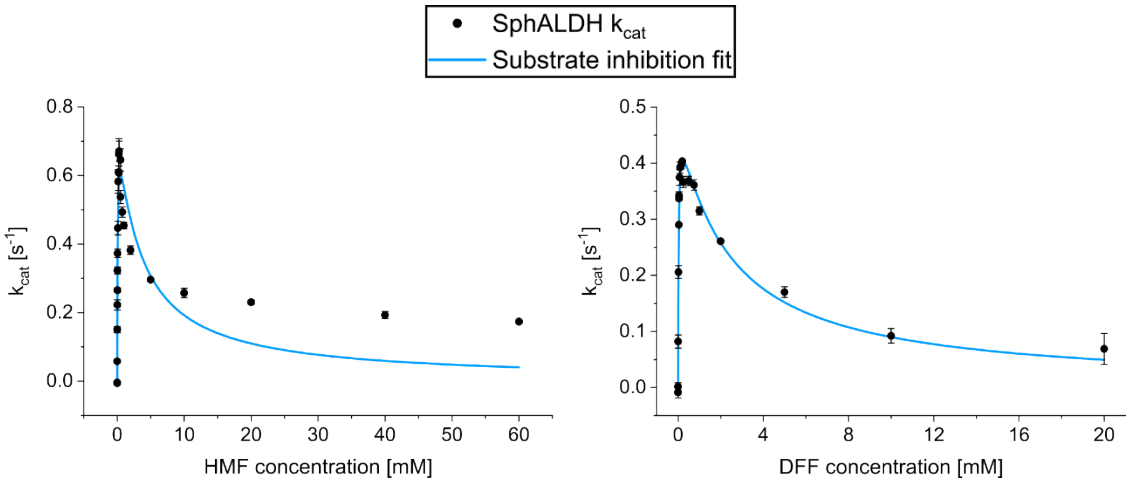

Figure S5. Enzyme kinetics of *Sph*ALDH on HMF and DFF.

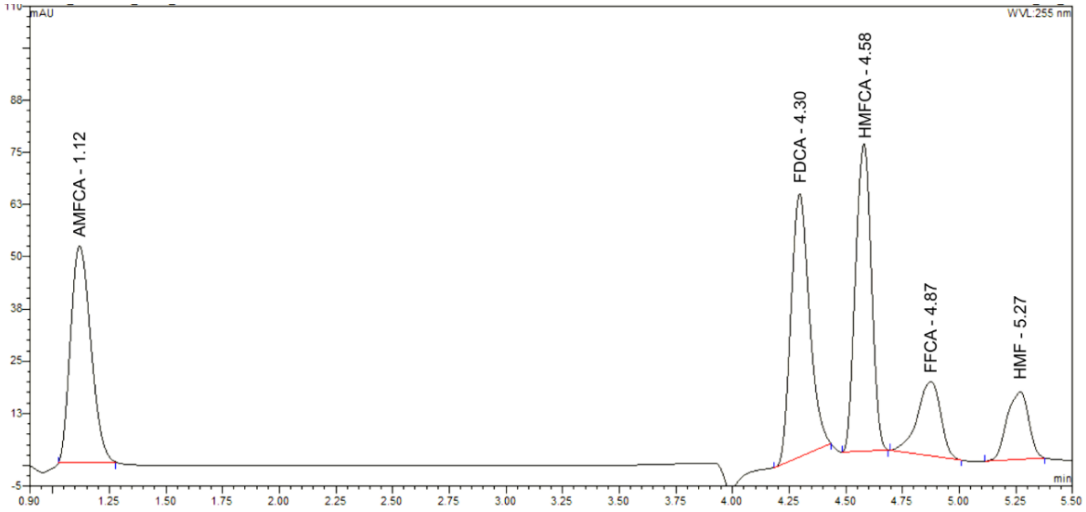

Figure S6. HPLC chromatogram of standards. Signal recorded at UV wavelength 255 nm.

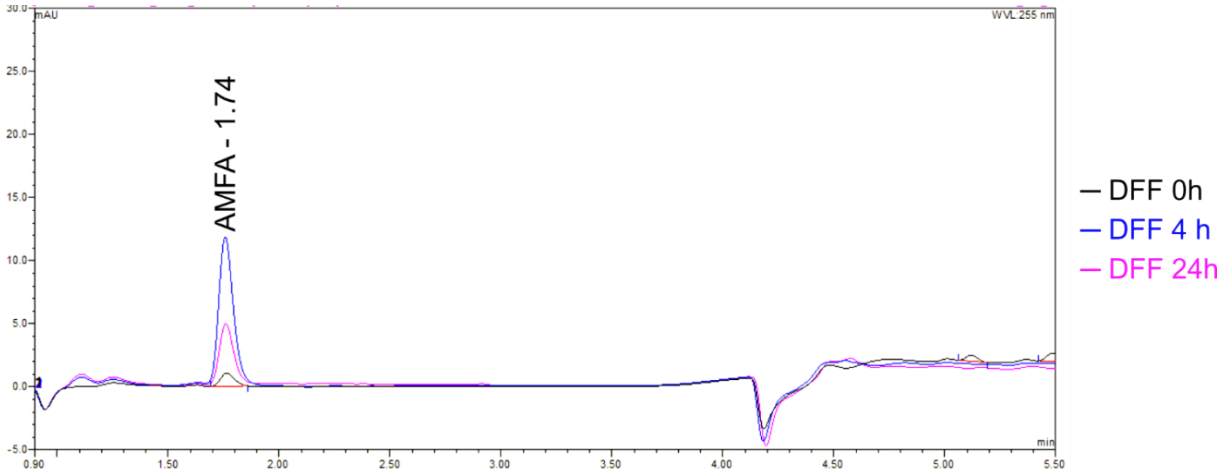

Figure S7. HPLC chromatograms (255 nm) of reactions for the direct amination of DFF. Reaction composition: 5 mM DFF, 10 mM L-alanine, 0.5 mM NADH, 20 mM ammonium acetate, 20 mM sodium formate, 6.7 µM *Cv*-oTA, 0.11 µM *Bs*AlaDH, 0.83 µM *Cb*FDH. Reaction conditions: in 100 mM NaPi buffer (pH 8.0), 30 °C, constant oscillation on rocking shaker.

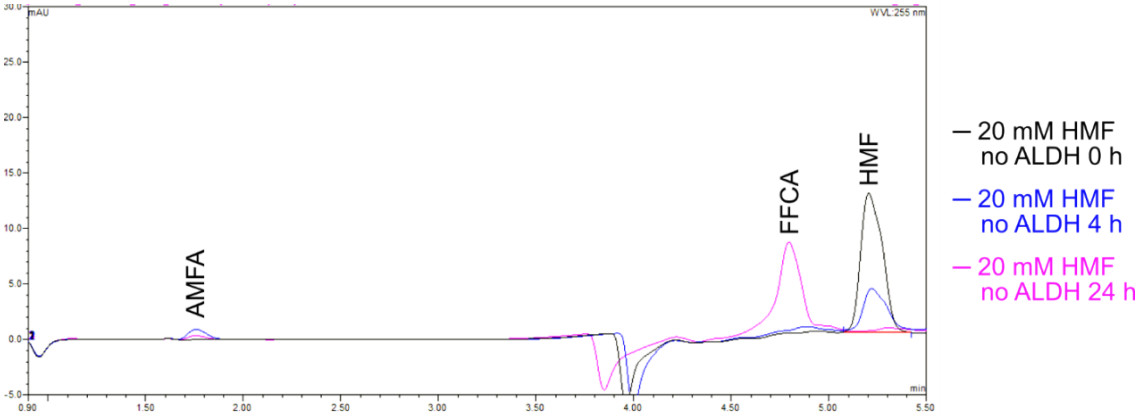

Figure S8. HPLC chromatograms (255 nm) of reactions presented in Figure 2d.

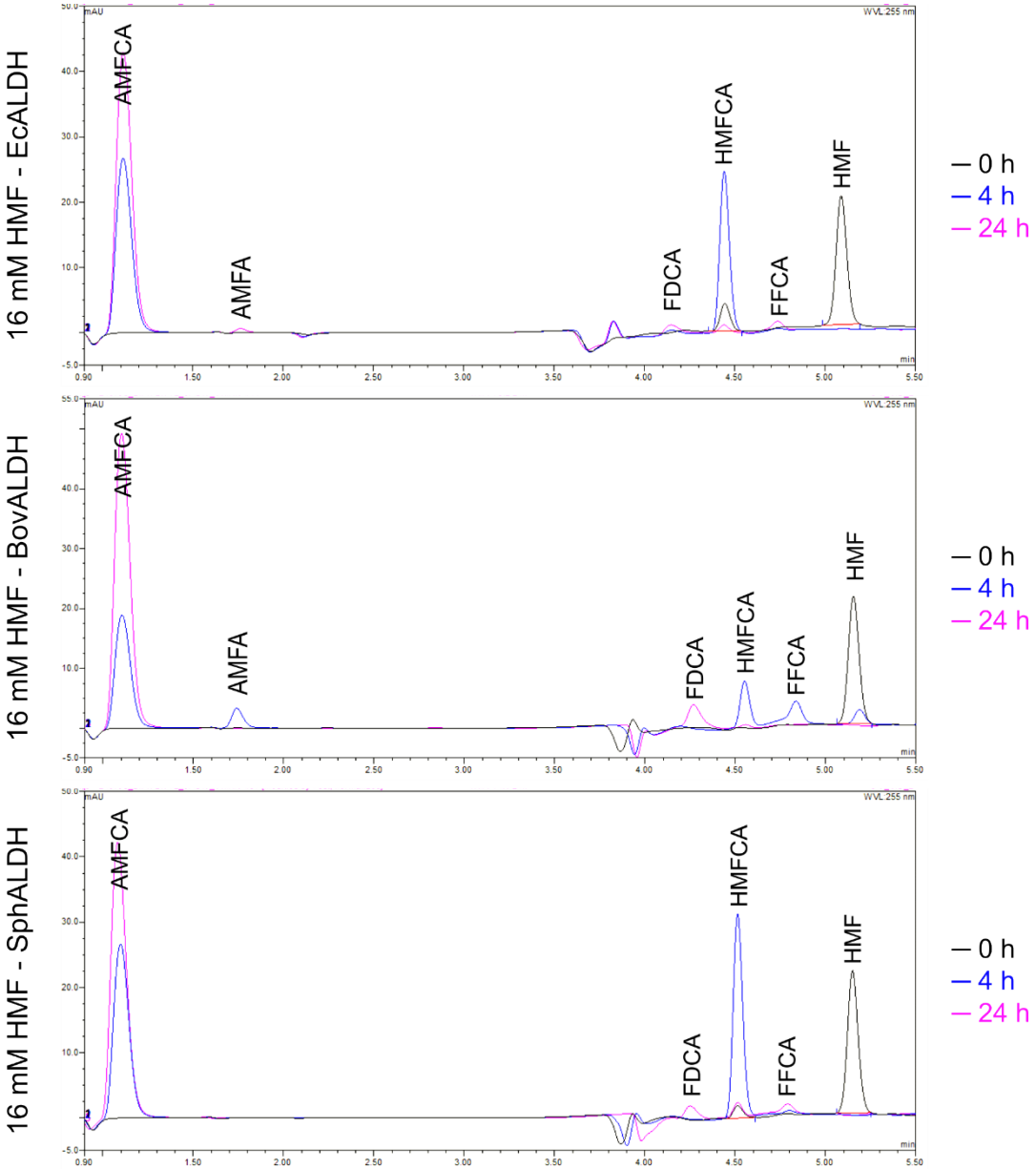

Figure S9. HPLC chromatograms (255 nm) of reactions presented in **Figure 2a** (16 mM HMF - *Ec*ALDH), **Figure 2b** (16 mM HMF - *Bov*ALDH) and **Figure 2c** (16 mM HMF - *Sph*ALDH).

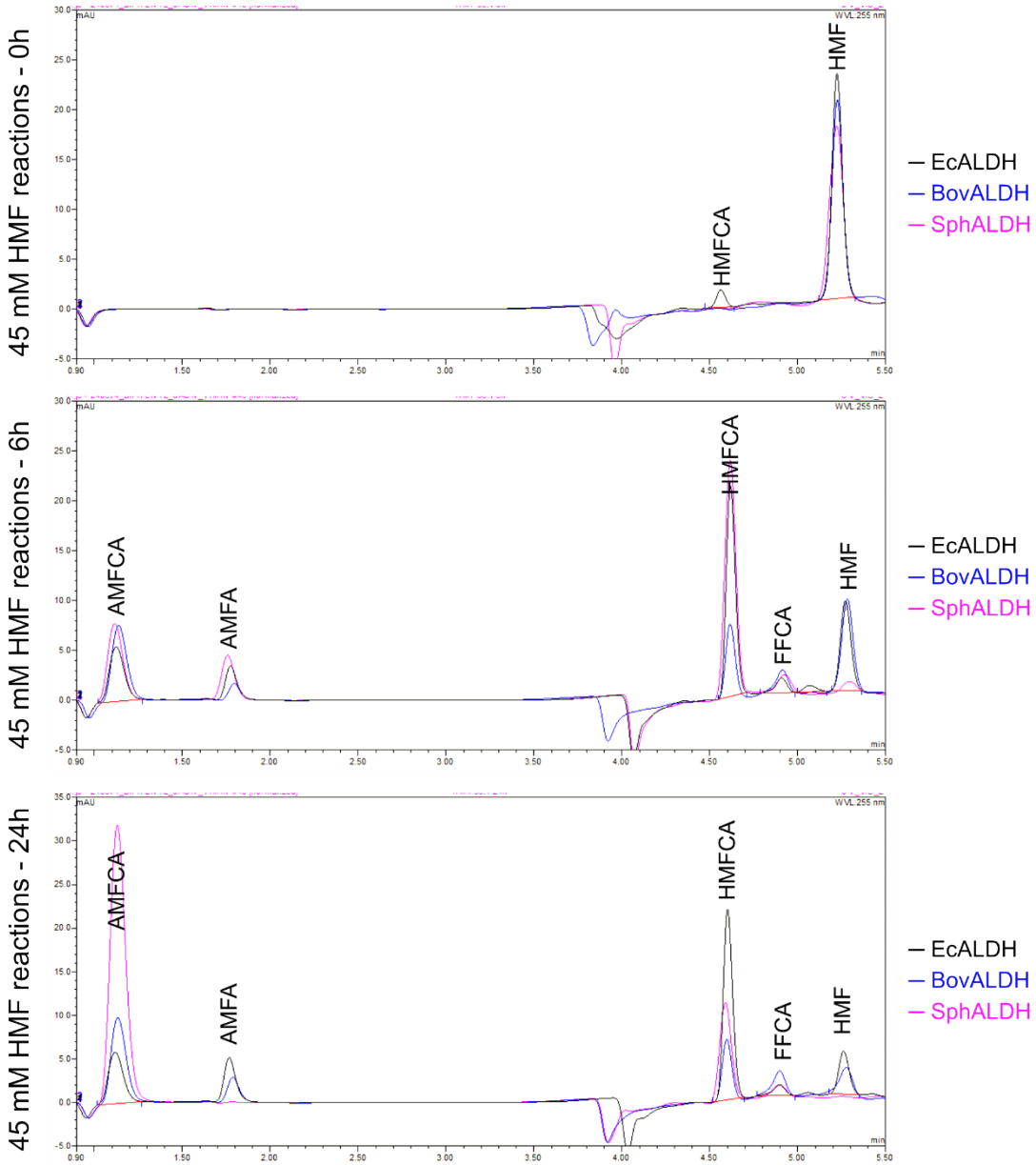

Figure S10. HPLC chromatograms (255 nm) of reactions presented in **Figure S3a** (45 mM HMF - *Ec*ALDH), **Figure S3b** (45 mM HMF - *Bov*ALDH) and **Figure S3c** (45 mM HMF - *Sph*ALDH).

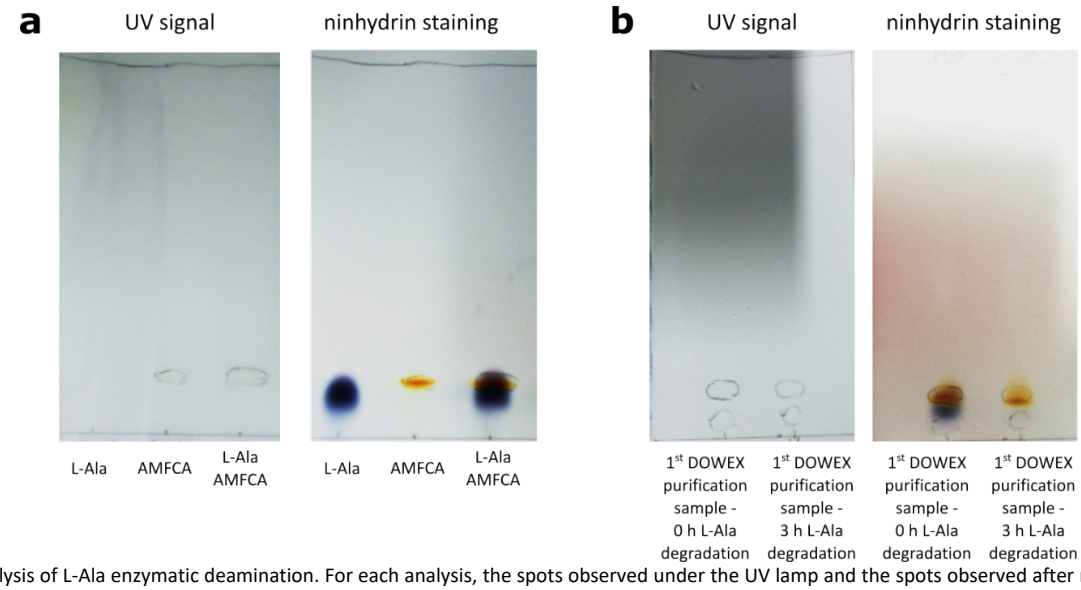

Figure S11. TLC analysis of L-Ala enzymatic deamination. For each analysis, the spots observed under the UV lamp and the spots observed after ninhydrin staining are reported. **a**: TLC analysis of L-Ala (50 mM in 100 mM NaPi buffer pH 8.0, 1 µL spot) and AMFCA (20 mM in 100 mM NaPi buffer pH 8.0, 1 µL spot) standards. **b**: TLC analysis of the L-Ala deamination in the solution containing the mixture of L-Ala and AMFCA obtained after the first DOWEX (cation exchanger) purification. 1 µL of L-Ala digestion solution was spotted per sample (0 h and 3 h).

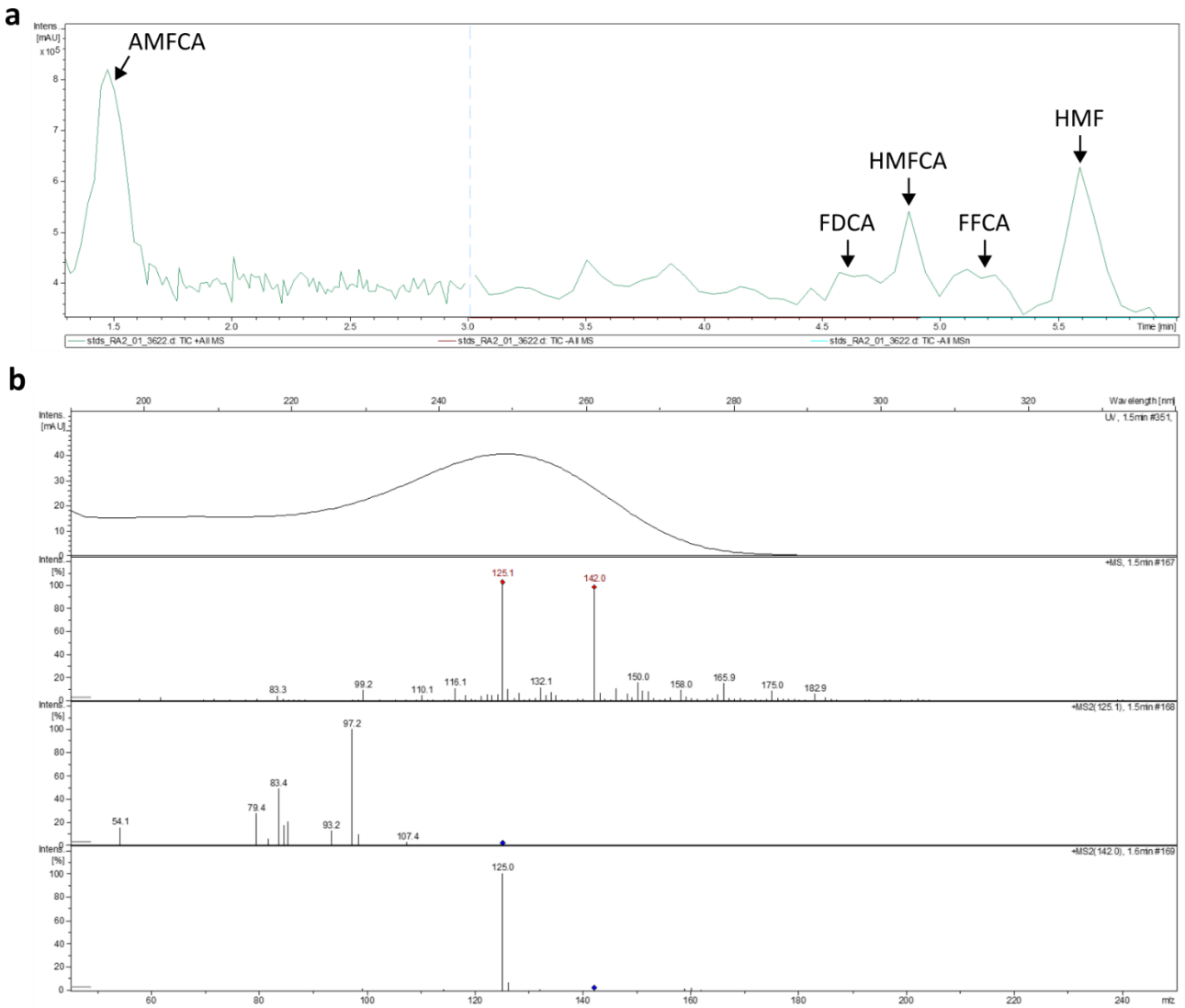

Figure S12. LC-MS analysis of furan derivatives standards (AMFCA, FDCA, HMFCA, FFCA, HMF, DFF). **a**: total ion chromatogram of LC-MS analysis. **b**: UV spectra, MS profile and fragmentation patterns of major masses (m/z = 142.0, m/z = 125.1) of AMFCA peak.

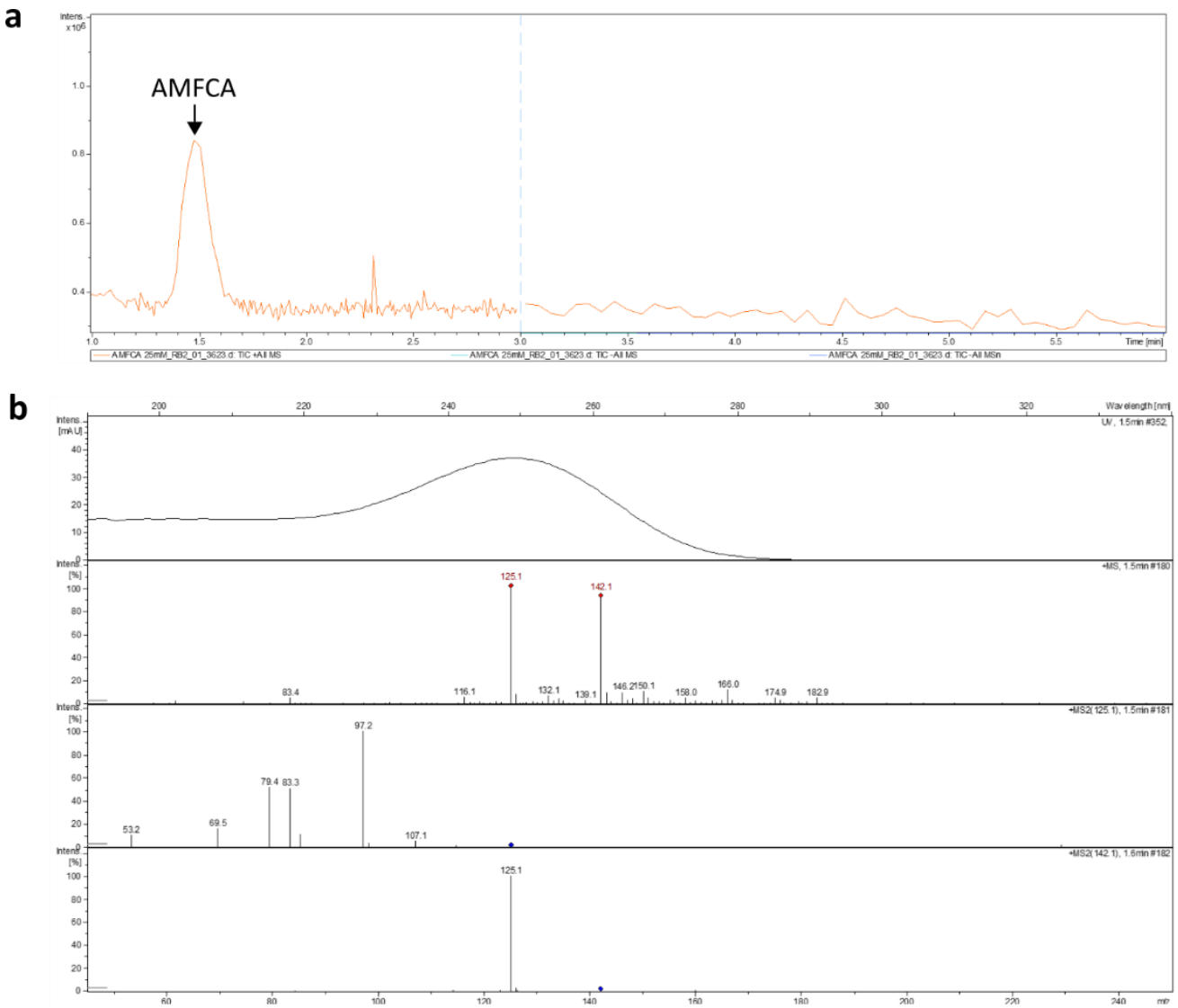

Figure S13. LC-MS analysis of purified AMFCA. **a**: total ion chromatogram of LC-MS analysis. **b**: UV spectra, MS profile and fragmentation patterns of major masses (m/z = 142.1, m/z = 125.1) of AMFCA peak.

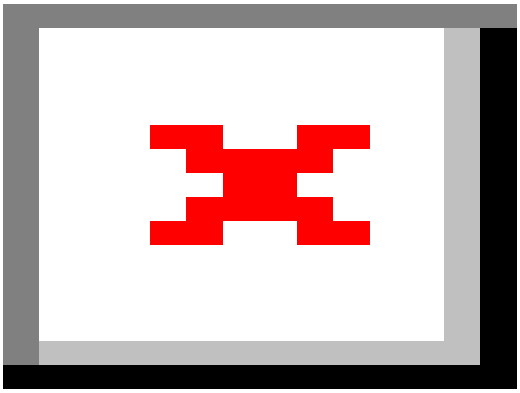

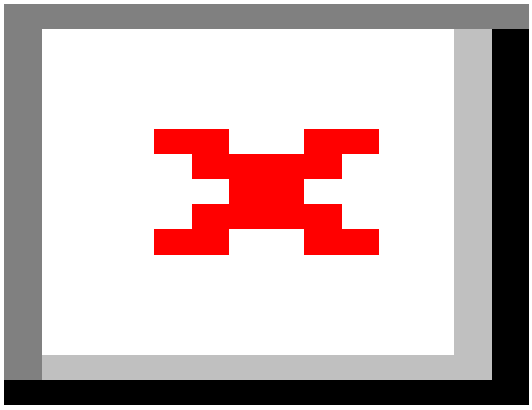

Figure S14. NMR analysis of purified AMFCA. H-NMR (above) and C-NMR (below).

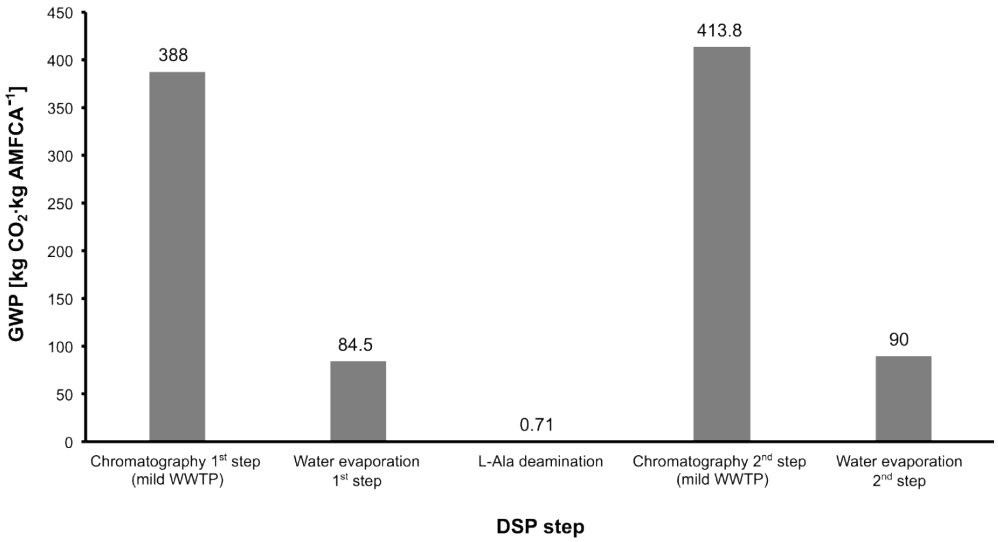

Figure S15. GWPs for each downstream process (DSP) step of AMFCA purification. The wastewater treatment for chromatography purification were considered “mild WWTP”. The water evaporation steps to obtain dry AMFCA powders were approximated to distillations for GWP calculations.

5. References

1. W. P. Dijkman and M. W. Fraaije, *Applied and Environmental Microbiology*, 2014, **80**, 1082-1090.
2. M. Sayed, Y. Gaber, F. Junghus, E. V. Martin, S. H. Pyo and R. Hatti-Kaul, *Microbial Biotechnology*, 2022, **15**, 2176-2190.
3. K. E. Cassimjee, C. Branneby, V. Abedi, A. Wells and P. Berglund, *Chemical Communications*, 2010, **46**, 5569-5571.
4. V. P. Willers, M. Döring, B. Beer and V. Sieber, *Chem Catalysis*, 2023, **3**.
5. S. Sutiono, A. Pick and V. Sieber, *Green Chemistry*, 2021, **23**, 3656-3663.
6. J. E. Jo, S. Mohan Raj, C. Rathnasingh, E. Selvakumar, W. C. Jung and S. Park, *Applied Microbiology and Biotechnology*, 2008, **81**, 51-60.
7. J. C. Saari, R. J. Champer, M. A. Asson-Batres, G. G. Garwin, J. Huang, J. W. Crabb and A. H. Milam, *Visual Neuroscience*, 1995, **12**, 263-272.
8. N. Kamimura, T. Goto, K. Takahashi, D. Kasai, Y. Otsuka, M. Nakamura, Y. Katayama, M. Fukuda and E. Masai, *Scientific Reports*, 2017, **7**, 44422.
9. W. P. Dijkman, C. Binda, M. W. Fraaije and A. Mattevi, *ACS Catalysis*, 2015, **5**, 1833-1839.
10. C. Nowak, B. Beer, A. Pick, T. Roth, P. Lommes and V. Sieber, *Frontiers in Microbiology*, 2015, **6**, 957.
11. C. Engler, R. Kandzia and S. Marillonnet, *PLoS One*, 2008, **3**, e3647.
12. D. G. Gibson, L. Young, R. Y. Chuang, J. C. Venter, C. A. Hutchison, 3rd and H. O. Smith, *Nature Methods*, 2009, **6**, 343-345.
13. K. Miyata, M. Miyashita, R. Nose, Y. Otake and H. Miyagawa, *Bioscience, Biotechnology, and Biochemistry*, 2006, **70**, 2138-2144.
14. P. Domínguez de María, *RSC Sustainability*, 2024, **2**, 3817-3825.
15. E. E. Agency, Greenhouse gas emission intensity of electricity generation, https://www.eea.europa.eu/en/analysis/maps-and-charts/co2-emission-intensity-15?activeTab=570bee2d-1316-48cf-adde-4b640f92119b, (accessed 10.03.2025).